I&EC research
Industrial & Engineering Chemistry Research

Article

Cite This: Ind. Eng. Chem. Res. 2019, 58, 1635−1649

pubs.acs.org/IECR

# From Batch to Continuous: Freeze-Drying of Suspended Vials for Pharmaceuticals in Unit-Doses

Luigi C. Capozzi,[†] Bernhardt L. Trout,[‡] and Roberto Pisano*[,†]

[†]Department of Applied Science and Technology, Politecnico di Torino, corso Duca degli Abruzzi 24, 10129 Torino, Italy
[‡]Department of Chemical Engineering, Massachusetts Institute of Technology, 77 Massachusetts Avenue, Cambridge, Massachusetts 02139, United States

Supporting Information

**ABSTRACT:** In response to the current trend in the pharmaceutical industry, a new concept for the freeze-drying of pharmaceuticals in unit-doses is presented: the continuous freeze-drying/lyophilization of suspended vials. This configuration makes it possible to set up a continuous freeze-drying process that produces a final product with similar characteristics to those traditionally obtained by means of the batch process but which avoids the drawbacks of conventional, batch freeze-drying. The feasibility and advantages of this new concept are presented in this work. Continuous freeze-drying has been found to improve heat transfer uniformity and reduce the primary drying duration by 2−4 times. As far as the structure of lyophilized products is concerned, SEM micrographs of the lyophilized samples showed that this technology improves vial-to-vial and intravial homogeneity.

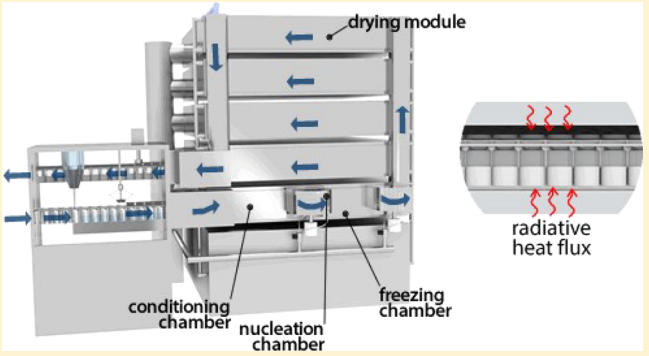


## INTRODUCTION

Although continuous manufacturing is a well-established practice in some industries, this approach is still relatively new to the pharmaceutical industry, where only 5% of manufacturing processes operate in continuous mode.[1] In this perspective, regulatory authorities, such as the U.S.A. Food and Drug Administration (FDA), the European Medicines Agency (EMA), and the Pharmaceuticals and Medical Devices Agency (PMDA) are promoting the integration of continuous manufacturing for pharmaceutical production.[2] The FDA is strongly encouraging the modernization of pharmaceutical manufacturing, with particular emphasis on Pharmaceutical Quality Systems (PQS), Quality by Design (QbD), Process Analytical Technology (PAT), and Real Time Release Testing (RTRT) and, of course, continuous manufacturing.[3] As far as this technology is concerned, the FDA has formally encouraged the pharmaceutical community to move toward continuous processing in order to improve efficiency and manage variability.[4,5] In 2016, the US government's National Science and Technology Council (NSTC) included continuous manufacturing of pharmaceuticals among the priority objectives of the US industry, and as a candidate for Federal investment and public-private collaborations.[6] Although there is no EU initiative that subsidizes continuous manufacturing in the pharmaceutical industry, EMA has repeatedly confirmed its favorable position on innovation in manufacturing and specifically on continuous approaches.[7] In Japan, PMDA is encouraging industry to introduce innovative continuous manufacturing technologies, based on science- and risk-based approaches.[8]

A number of potential processes already exist that can significantly benefit from shifting from batch to continuous productions,[9−15] and a growing number of manufacturers have recently been converting their processes to adopt continuous production for their commercial drugs. Vertex has been using a continuous manufacturing technology for the production of the cystic fibrosis drug tablets, Orkambi, since 2015.[16] In 2016, the FDA approved the switching from batch to continuous manufacturing of Prezista, a drug in tablet form produced by Janssen Supply Chain for the treatment of HIV-1 infection.[5] This conversion to continuous was the result of a partnership between the Janssen Supply Chain with Rutgers University, the University of Puerto Rico, and the Engineering Research Center for Structured Organic Particulate Systems (C-SOPS). A further example of a commercial drug produced by continuous manufacturing and already available on the market is Severin, a nimesulide tablet produced by Chinoin.[17,18] In addition to these private initiatives, many pharmaceutical companies have increased their efforts to develop new continuous processes in collaboration with universities. Novartis-MIT Center for Continuous Manufacturing, a 10-year research collaboration project between Novartis and the

Received: June 27, 2018
Revised: December 14, 2018
Accepted: January 4, 2019
Published: January 4, 2019






DOI: 10.1021/acs.iecr.8b02886
Ind. Eng. Chem. Res. 2019, 58, 1635−1649

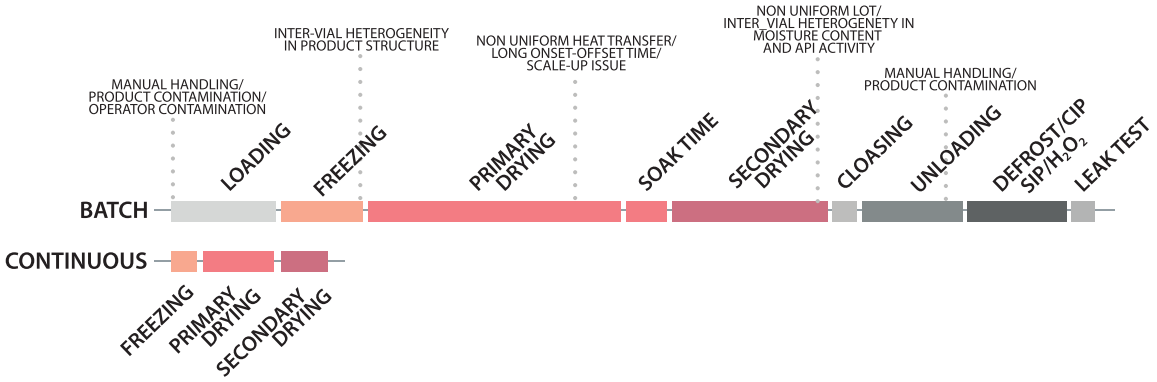


**Figure 1.** Timeline for the batch and continuous lyophilization strategies.

Massachusetts Institute of Technology (MIT), developed a fully integrated, continuous manufacturing plant to synthesize Aliskiren and produce coated tablets.[19] In Europe, the Centre for Innovative Manufacturing for Continuous Manufacturing and Crystallization (CMAC) at the University of Strathclyde is collaborating with several industries to develop new continuous processes. Other initiatives are ongoing in Singapore, where GlaxoSmithKline is building a continuous manufacturing plant for antibiotic production[20] and Amgen introduced a continuous purification process into its production line.

While much attention has been dedicated to the advancement of continuous manufacturing, the freeze-drying community is making extensive efforts to improve process robustness and achieve the stringent requirements of quality, safety, and efficiency set by regulatory authorities. In this perspective, research on freeze-drying has mainly focused on process control, monitoring,[21−27] optimization,[28] and scaling-up.[29] Many efforts have been made to improve the quality and uniformity of the product,[30,31] as well as on the development of cycles that guarantee the stability of APIs.[32] Despite these efforts, conventional freeze-drying still presents serious limitations[33] that call for a change in the mindset, that is, to shift from conventional batch processes to innovative, continuous, modular ones. It is clear that freeze-drying needs to be completely rethought in order to be better integrated in the drug production chain and more flexible to respond to variations in market needs as well as to allow the online monitoring of product quality and overcome batch-to-batch variability.[34,35]

Over the past decades, many ideas regarding continuous freeze-drying have been proposed, but none of them has yet been successfully applied in the industry.[36,37] In fact, these technologies do not allow either a perfect, precise control of product quality, or guarantee the sterility of the product and, in the case of particle-based products, can potentially lead to safety problems, due to the exposure of operators to microparticles or allergenic dust in the air. New technologies have recently been proposed, i.e., active freeze-drying,[38] fine-spray freeze-drying,[39] and spin-freezing and radiative drying.[40,41] Although these processes increase the efficiency of freeze-drying, some issues and concerns still remain, especially due to the lack of control and standardization of the dried products. For example, ice nucleation temperature, and thus product morphology, cannot be controlled and remains stochastically distributed. Notwithstanding, spin freezing can manipulate temperature and flow rate of the cryogenic gas and thus control cooling at individual vial level. However, the final product obtainable using the previous technologies is different from the traditional pharmaceutical dosage form of lyophilized products and may represent a further obstacle to their implementation in industry.

In this work, a new concept for the freeze-drying of pharmaceuticals in unit-doses is presented and evaluated, namely the continuous freeze-drying of suspended vials. The continuous flow of vials is reached by suspending vials and moving them through chambers kept at controlled temperatures and under controlled pressure conditions. In this paper, we propose a new technology to perform continuous freeze-drying and briefly describe the working principle and the apparatus. The feasibility of this new concept has been demonstrated by replicating the condition of the continuous process in a functional prototype.

## ■ DRAWBACKS OF BATCH FREEZE-DRYING

Conventional pharmaceutical freeze-drying is a batch-wise process consisting of three main stages, that is, freezing, primary drying, and secondary drying. Each stage suffers from particular drawbacks, which are discussed in detail below. Moreover, there are other time-consuming operations, such as (a) vial filling, (b) vial loading and unloading, (c) cleaning in place, (d) sterilization in place, (e) filter integrity test, (f) the leak test, and (g) defrosting. At this stage, we have not taken into consideration the downtimes resulting from these ancillary operations. As shown in Figure 1, these operations can represent more than 50% of the whole process and can decrease process efficiency and profitability.

**Freezing.** Freezing plays a central role in the lyophilization of pharmaceuticals, because it determines the final structure of the dried product,[42,43] affects the composition of the polymorphs and the stability of many APIs,[44] and influences the duration of the drying stage and the final moisture content in the dried product.[30,45,46] Vials are filled with a predefined volume of the drug solution and then placed directly on the shelf. Once the vials have been loaded into the chamber, the shelf temperature is reduced below the equilibrium freezing temperature. The freezing protocol can be designed on the basis of historical data available for similar formulations or using more recent model-based approaches.[29,47] During freezing, the mechanisms involved in the heat transfer between the heat transfer fluid and the product in the vial are mainly the conduction through air within the gap between the vial and the shelf, radiation from the shelf and the surrounding area, contact between the shelf and the vial, and the natural convection of air around the side of the vial. As shown in a


DOI: 10.1021/acs.iecr.8b02886
Ind. Eng. Chem. Res. 2019, 58, 1635−1649

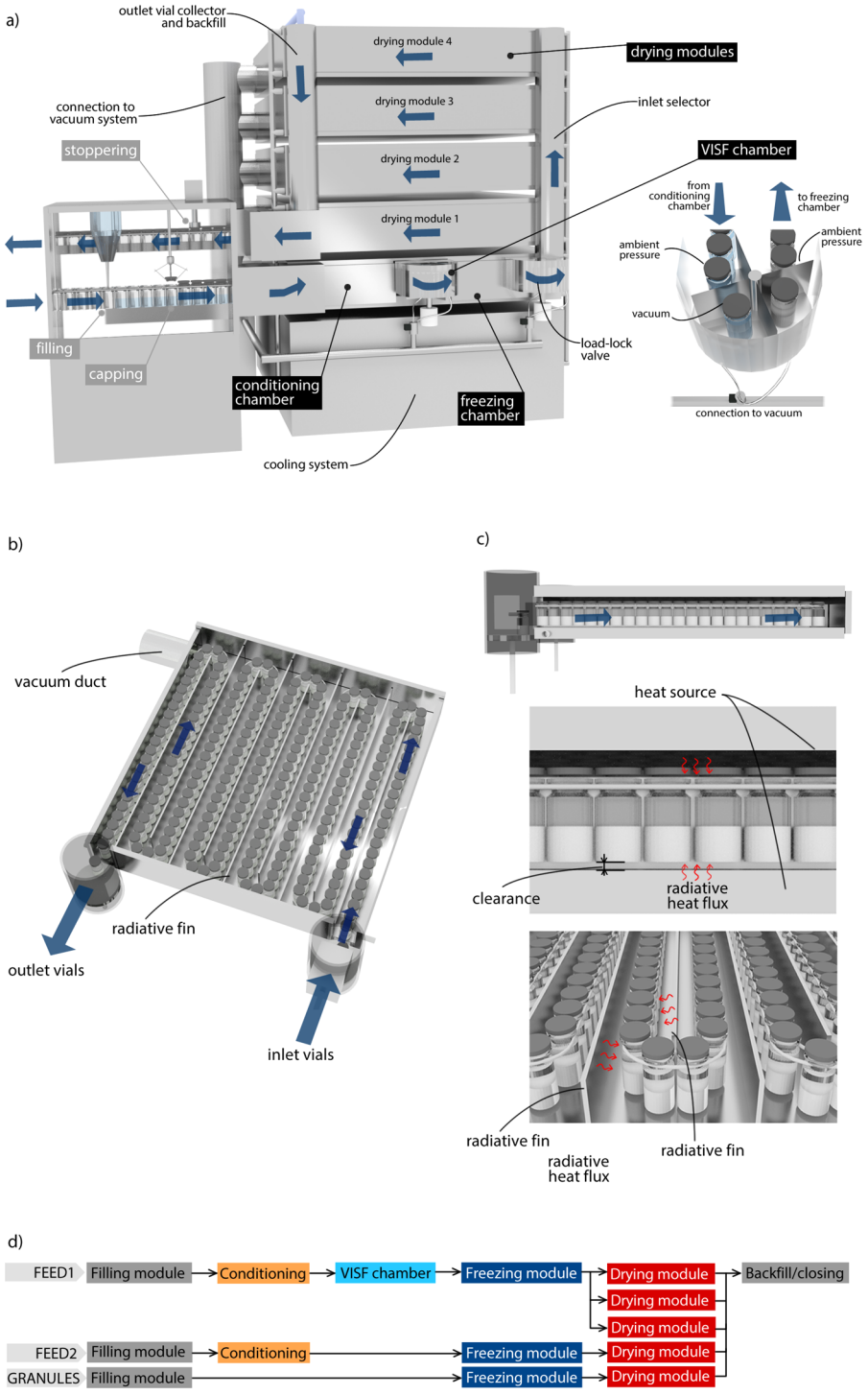


**Figure 2.** Schematic of (a) the continuous freeze-dryer and (b) a drying module. The front view of the drying module (c) and examples of potential configurations for the continuous lyophilizer (d) are also shown. The estimated chamber volume of the continuous lyophilizer (including both freezing and drying modules) is approximately 0.7 $m^3$.

previous work,[48] the contribution of gas conduction is much higher than the other previously mentioned mechanisms and represents about 90% of the whole transferred heat. During freezing, the temperature of the product should have an intermediate value between the shelf temperature and that of the surrounding area. Therefore, while the temperature-controlled shelf cools down the product, heat is supplied to the side of the vial. This configuration thus leads to higher temperature gradients within the product and increases the heterogeneity of its frozen structure.

**Primary and Secondary Drying.** During primary drying, the key variables that have to be controlled are the product temperature and drying time. The product temperature has to be maintained below a limit value to satisfy the product quality requirements, while the drying time has to be long enough to ensure that ice sublimation is completed in all the batch vials.



DOI: 10.1021/acs.iecr.8b02886
*Ind. Eng. Chem. Res.* 2019, 58, 1635−1649

These process parameters can be controlled directly by manipulating the shelf temperature and chamber pressure.

In batch freeze-drying, vials are in direct contact with the shelves and occupy different positions within the chamber. The heat flux between the shelf and vials results from various mechanisms and depends on the geometry of the equipment and container, as well as on the pressure and temperature of both the shelves and the surroundings.[49] In batch freeze-drying, heat is supplied by (i) direct conduction from the shelf to the glass at the points of contact, (ii) conduction through the gas in the gap at the bottom of the vial, and (iii) radiation from the lower and upper shelves and from the surroundings, i.e., chamber walls and door.

As shown by Ganguly et al.,[50] direct contact contributes to 10−40% of the total heat transferred, depending on the temperature and pressure conditions, and represents an important cause of nonuniformity in the heat transfer rates. In fact, as estimated by means of a print test, this contact surface is only a small fraction of the cross section of the vial[51] and its extension essentially depends on the type of vial but also on how flat the shelf surface is.

The second contribution to heat transfer is conduction through the gas in the gap between the shelf and the vial bottom, which depends on the pressure but also on the curvature of the vial bottom. This contribution also represents a serious cause of nonuniformity of the heat transfer, due to the variability in the curvature of the vial bottom.[52]

The third contribution to the heat flux is a result of radiation from the lower and upper shelves, as well as from the chamber walls and door. This contribution is generally the most relevant cause of heat transfer nonuniformity.[49,53] In fact, although vials located in the center of the shelf receive radiative heat from the bottom and upper shelves, vials located at the side of the batch also receive radiative heat from the chamber walls and/or door. This effect is known as the edge-vial effect and represents a serious problem during cycle scale-up and for the process control itself.[54] Pisano et al.[49] in fact observed that the heat transfer coefficient of vials in the corner of the chamber, which are those most affected by radiation from the chamber walls or door, is approximately twice that of the vials in the central part of the batch. Similarly, the product temperature of the edge vials is much higher than that observed for central vials.[55−57]

Another cause of heterogeneity in heat transfer is the temperature gradient over the shelf. In fact, the heat transfer fluid passes through the internal flow channel of the shelves and heats the products. In a pilot-scale lyophilizer under full-load conditions, the inlet−outlet temperature difference can be of the order of magnitude of 1−2 K, but this difference can be much greater in an industrial-scale lyophilizer. Cheng et al.[58] estimated a temperature gradient of between 0.02 and 0.07 K $cm^{-1}$ along the shelf.

The nonuniformity of pressure in the lyophilizer chamber is also a cause of heterogeneity in the batch, in terms of drying rate and maximum temperature reached by the product during primary drying. As shown in refs 55, 59, and 60, this effect is not negligible and determines a further uncertainty in the control of the process as well as important implications on the final quality of the product.

## CONTINUOUS FREEZE-DRYING CONCEPT

The continuous lyophilizer is composed of a sequence of modules, each of which is dedicated to a different operation, i.e., freezing or primary and secondary drying, and are connected one to another to guarantee continuity of the heating vial flow and so as to be perfectly integrated with the downstream processes. The continuous flow of vials is achieved by suspending the vials over a track and moving them through chambers that have different conditions, pressures, and temperatures and which are separated by a load-lock system. A load-lock system is a special device used to transfer vials between modules operating at different pressure and temperature. This configuration makes the freezing and drying operations continuous. A schematic of the equipment is shown in Figure 2.

As can be seen in Figure 2d, through the modular design of the equipment, it is possible to implement various freezing methods or dosage forms (bulk and particle-based materials) and easily increase throughput by enabling one or more modules working in parallel. Such a modular system is particularly suited for modern markets where the speed and flexibility of production is a crucial element.

**Filling and Load-Lock Systems.** The first step of the process is the continuous filling and loading of vials. This operation is naturally continuous and is already used in batch freeze-drying. Unfortunately, filling represents an unavoidable dead time in batch freeze-drying, although an automatic filler can process 30,000 vials per hour. On the other hand, in the case of continuous mode, this operation does not require high-speed filling equipment, since vials are continuously loaded into the equipment. Similarly, in the case of particle-based products, the frozen particles are continuously filled into vials and loaded, one by one, into the equipment. A fully automated system provides a sufficient number of vials per minute to feed the freezing modules. This operation is carried out in a sterilized and temperature controlled environment to avoid contamination and deactivation of the APIs.

Once filled, the vials are partially stoppered and then continuously loaded into the apparatus though a load-lock system. Various configurations for load-lock systems are currently under investigation. All these configurations are basically based on the same operating principle that is described herein. At the end of each module, the vial is picked up and is transferred into an intermediate chamber. As the vial is transferred into the intermediate chamber, this chamber is isolated from the first module. After that, the pressure is reduced through a vacuum pump or increased by introducing a controlled flow rate of sterile gas at atmospheric pressure. Once the same pressure of the second module has been reached, the intermediate chamber is opened and the vials is transferred into the second module. Then, the intermediate chamber is closed, the pressure is adjusted according to that of the first module, and finally is reopened.

**Freezing Module.** As shown in Figure 2, the vial is filled with a predefined volume of liquid or frozen particles and then transferred, through a load-lock system, to the freezing module. Here, the vessels are suspended and moved over a moving track.

The freezing module consists of three submodules: (A) a conditioning module, (B) a load-lock system, where controlled nucleation can eventually take place, and (C) an equilibration/freezing module. The operations that the continuous freeze-dryer has to carry out depend on the dosage form of the product that has to be freeze-dried.

In the case of particle-based products, after filling, each vial is moved into the conditioning chamber and then directly into drying modules.



DOI: 10.1021/acs.iecr.8b02886
Ind. Eng. Chem. Res. 2019, 58, 1635−1649

For liquid solutions, the vial is cooled and equilibrated to the desired temperature by adjusting the temperature and flow rate of the cryogenic gas in the conditioning module. The vial then enters the load-lock system, where it is exposed to a vacuum that induces nucleation and is, then, transferred to the freezing module, where its temperature is lowered and the solidification of the solution is completed. This operation is used to perform vacuum-induced surface freezing (VISF) in continuous mode, but the equipment can generally also perform uncontrolled nucleation.

*Conditioning Chamber.* In the conditioning module, vials are conditioned to the desired temperature by flowing the cryogenic gas, nitrogen or another gas, at a controlled temperature and flow rate. Vials are suspended over a moving track and moved along the module. The temperature and flow rate of the cryogenic fluid have to be adjusted to ensure that the vials reach their desired temperature before exiting from the module.

The preconditioning of the product that has to be freeze-dried is always compulsory in the case of VISF, but it is also suggested in the case of uncontrolled nucleation in order to improve product homogeneity.

*Control of the Nucleation Temperature.* The control of the nucleation temperature is essential to make both the drying behavior and product morphology uniform. Various methods are available to control the nucleation temperature, e.g., ultrasounds, ice fog, and pressure disturbance. All these methods can be integrated into the present technology, but we here propose the application of VISF technology, which uses the vacuum to instantaneously induce the nucleation event. VISF can easily be adapted, and it can be carried out directly in the load-lock systems used to load the vial into the freezing module. In fact, nucleation is induced by reducing the pressure directly inside the load-lock chamber; this pressure reduction promotes the partial evaporation of the solvent and hence cools the solution, thus facilitating the formation of stable nuclei. This method guarantees the replication of the nucleation temperature in the vials and, thus, of an ice morphology.

*Freezing Chamber.* In the freezing modules, vials are cooled by forced gas circulation until complete solidification of the product occurs. In this module, heat is prevalently transferred by gas convection and radiation from the surroundings.

In order to speed up and make the heat transfer between the equipment and the vessel more uniform, the cryogenic fluid can be forced to move along the freezing module, in a similar way to as in the conditioning chamber. In this manner, the external surfaces of the vials are flushed to the same extent by the cryogenic gas, thus reducing the heterogeneity of the heat flux that usually occurs in conventional batch freezing, where vials are loaded onto temperature-controlled shelves and receive different amounts of heat, depending on their position on the shelf.

Different freezing protocols can be performed by modulating the velocity of the cryogenic fluid and its temperature; moreover, these two process parameters can be adjusted to control the duration of the freezing and, thus, to design the final structure of the product.

**Primary and Secondary Drying Module.** This module is connected to a vacuum system, condenser, and vacuum pump, which guarantees the desired pressure, while the temperature of the equipment surfaces is controlled by adjusting the temperature of the heat transfer fluid, that is, silicon oil, by means of a refrigeration system. In this configuration, the vials are not in contact with the shelves, and heat is essentially transferred by radiation. In fact, a low pressure, below 1 mbar, makes the heat transfer by convection and conduction negligible, with respect to the radiative contribution. This configuration allows the heat to be uniformly transferred to the vessel, thus avoiding those problems that are typical of batch freeze-drying, where individual vials behave differently, depending on their position within the batch and because of variations in the geometry of the vials themselves. Furthermore, the temperature and pressure gradients within the equipment no longer represent a cause of heterogeneity in the heat transfer, because the vials, following the same path, are exposed to exactly the same conditions. However, various designs of the drying module are currently under investigation in order to minimize its resistance to vapor flow and thus avoid any significant pressure drop over the module.

It can be claimed that each vial can partially shadow the adjacent vials at the points of contact and thus restrict radiant heat transfer from the environment. However, the shadowing of one vial by its neighbors does not significantly impact on the fraction of radiant energy that leaves the temperature-controlled surfaces of the equipment and reaches the vial. This is particularly true for the geometric arrangement of array of vials shown in Figure 2 where radiant heat comes from all sides of the chamber. In any case, even if the radiant heat is not uniformly transferred to each vial, then it tends to be uniformly distributed within the product by conduction through the vial wall and the frozen product as well.

As the vials move through the equipment, they are in contact with each other; however, the direct contact contribution to heat transfer should be negligible since the temperature gradient between adjacent vials is small, smaller than 0.5 K. By contrast, this contribution might be not negligible in a batch of vials where, e.g., the temperature gradient between edge-vials and the adjacent ones can be of 1−3 K.

In this module, heat is supplied by radiation through temperature-controlled surfaces but can potentially be transferred using other technologies, such as IR radiation or microwaves. As heat is essentially transferred by radiation, the control of the temperature of the product being dried is much easier, and this allows uniformity in the heat transfer to be guaranteed and, thus, in the drying behavior.

The same equipment configuration is suitable for both the primary and secondary drying modules; the two modules are thus identical but operate at different pressures and temperatures.

## MATERIALS AND METHODS

**Experimental Setup.** A functional prototype has been used to reproduce the same conditions that occur in the here proposed continuous process and to study the heat transfer process during freezing and primary drying, as well as their effect on the product quality and characteristics. Various process conditions have been investigated to better understand the range of applicability of this new technology. It should be pointed out that, in this functional version of the continuous lyophilizer, vials do not move along the plant, but undergo similar heat and mass transfer conditions to those of a continuous plant. We investigated the following configurations:

(A) batch freeze-drying, uncontrolled freezing



DOI: 10.1021/acs.iecr.8b02886
Ind. Eng. Chem. Res. 2019, 58, 1635−1649

Table 1. List of the Experiments Carried out to Compare the Batch and Continuous Freeze-Drying Modes

| test | solution | | configuration | nucleation | $T_s$, K | $P_c$, Pa |
|---|---|---|---|---|---|---|
| 1 | 5% mannitol | (A) | batch | spontaneuous | 263 | 10 |
| 2 | 5% mannitol | (B) | contact+radiation | spontaneuous | 263 | 10 |
| 3 | 5% mannitol | (C) | suspended | spontaneuous | 263 | 10 |
| 4 | 5% mannitol | (C) | suspended | spontaneuous | 293 | 4 |
| 5 | 5% mannitol | (C) | suspended | spontaneuous | 298 | 2 |
| 6 | 5% mannitol | (E) | suspended | VISF ($T_n$ = 268 K) | 263 | 3 |
| 7 | 5% mannitol | (E) | suspended | VISF ($T_n$ = 268 K) | 283 | 3 |
| 8 | 5% mannitol | (E) | suspended | VISF ($T_n$ = 268 K) | 293 | 3 |
| 9 | 5% mannitol | (E) | suspended | VISF ($T_n$ = 268 K) | 313 | 3 |
| 10 | 5% mannitol | (A) | batch | spontaneuous | optimized | 10 |
| 11 | 5% mannitol | (D) | batch | VISF ($T_n$ = 268 K) | optimized | 10 |
| 12 | 5% sucrose | (A) | batch | spontaneuous | 253 | 10 |
| 13 | 5% sucrose | (E) | suspended | spontaneuous | 253 | 10 |
| 14 | 5% sucrose | (E) | suspended | spontaneuous | 273 | 2 |
| 15 | 5% sucrose | (E) | suspended | VISF ($T_n$ = 268 K) | 293 | 2 |

(B) batch freeze-drying of completely irradiated vials, uncontrolled freezing

(C) suspended-vial freeze-drying, uncontrolled freezing

(D) batch freeze-drying, controlled freezing

(E) suspended-vial freeze-drying, controlled freezing;

All of the experiments have been carried out in a special chamber where top and bottom surfaces were temperature-controlled and connected through vertical fins. Vials were suspended between the temperature-controlled shelves and underwent similar processing conditions to those that occur in a continuous lyophilizer (case C and E).The temperature gradient along the vertical fins was modest, few kelvins at 273 K. The chamber pressure was measured by means of a capacitance manometer (MKS Baratron Type 626a) and a thermo-conductive gauge (PSG-101-S, Infcon, Bad Ragaz, Switzerland). The ratio between these two pressure readings was used to detect the primary drying endpoint.

Experimental runs were carried using two formulations, that is, aqueous solutions of 5% (w/w) mannitol and 5% (w/w) sucrose. The solutions were prepared using water for injection (Fresenius Kabi Italia, Isola della Scala, Italy) and filtered using 0.2 $\mu$m filters. An aliquot of 3 mL of mannitol solution or 2 mL of sucrose solution was filled into tubing vials (10R 24.0 × 45.0, Nuova Ompi, Piombino Dese, Italy). Miniature thermocouples (T type, Tersid, Milano, Italy) were used to measure the product temperature as well as the temperature of the shelves, chamber walls, and the air temperature within the chamber.

Handmade supports were used to suspend the vials and simulate similar heat transfer conditions as those of a continuous process. Each support was made of a plexiglass track and was sustained by screw pillars. The neck of the vial was held securely by the track and the vial remained suspended and fixed in the same position. The screw pillars also allowed the height of the tracks to be adjusted and therefore the clearance between the shelf and the vial. In the case of the batch lyophilizer, thermocouples have been inserted into both edge and central vials since they usually undergo different heat transfer conditions and, thus, could exhibit different product temperature on constant processing conditions.

As can be observed in Table 1, various configurations were studied by varying the vial loading, considering batch vs continuous mode and uncontrolled versus controlled freezing.

Controlled nucleation was performed using VISF, as proposed by Oddone et al.,[26] see Figure 3. Once the vials had been loaded into the lyophilizer, the shelf temperature was decreased from room temperature to a given $T_{s,n}$ and was held for 1.5 h to stabilize the whole lot of vials at $T_n$. At this point, the pressure inside the chamber was reduced from ambient to a given pressure, i.e., 130 Pa for both 5% mannitol and 5% sucrose, thus inducing nucleation in all vials. As widely discussed in Oddone et al.[26] the pressure at which nucleation is induced has to be carefully selected so as to avoid any undesired phenomena such as boiling of the liquid being frozen. The pressure was then released to atmospheric pressure; the shelf temperature decreased to $T_{s,m}$ and was held at that temperature for 1.5 h, thus promoting ice crystal growth. The complete solidification of the product was achieved after lowering the shelf temperature to 228 K. $T_{s,n}$ and $T_{s,m}$ were set to 261 and 251 K, respectively, for both 5% mannitol and 5% sucrose, and this resulted in $T_n$ equal to 268 K, while the chamber pressure was 130 Pa.

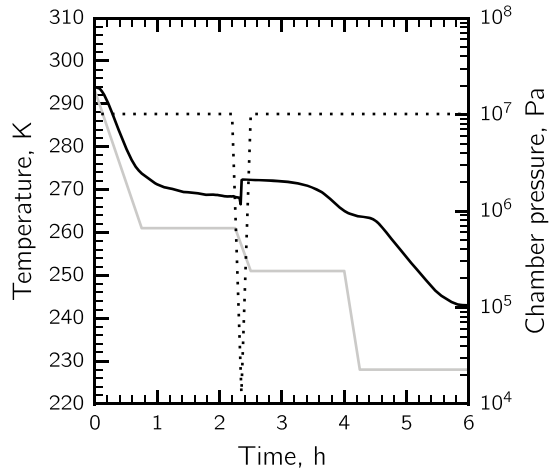


Figure 3. Evolution of the pressure (dashed line), shelf temperature (solid gray line), and product temperature (solid black line) when VISF is applied in the suspended-vial configuration.

**Characterization of the Heat Transfer and Mass Transfer for the Continuous Lyophilizer.** In the continuous lyophilizer, vials are not in contact with the



DOI: 10.1021/acs.iecr.8b02886
Ind. Eng. Chem. Res. 2019, 58, 1635−1649

temperature-controlled shelves, and heat is essentially transferred by radiation and convection.

Knowledge of the contribution of the various heat transfer mechanisms for the two plant configurations, that is, continuous vs batch, is thus essential to identify their potential advantages and disadvantages. This analysis has to be carried out for both freezing and drying (see the procedure used to calculate the heat power in the Supporting Information).

**Characterization of Lyophilized Products.** The porous structure of the dried product was analyzed using a scanning electron microscope (SEM, FEI type, Quanta Inspect 200, Eindhoven, The Netherlands); the samples were metalized and examined at 15 kV and under a high vacuum. The analysis was carried out at different points in the product (top, center, and bottom) to determine the intravial heterogeneity. The pore size distribution in the product was obtained from an analysis of the SEM images. A total of 50 to 150 pores were selected from each image and approximated as an ellipse; the pore dimension was calculated as the equivalent circle with the same area-to-perimeter ratio as that ellipse.

**Residual Moisture Analysis.** The Karl Fischer titration (Karl Fischer Moisture Meter CA-31, Mitsubishi, Japan) was used to determine the residual moisture content of the sample vials. Hydranal titration solvent (Sigma-Aldrich, Milano, Italy) was used in the case of sucrose, whereas formamide was added to those samples containing mannitol; the solution was then sonicated for 5 min. A titration blank was carried out to determine the moisture concentration in formamide which was then subtracted from the net amount of water in each sample.

In the case of sucrose-based solutions, moisture content was analyzed for the batch cycle (test 12) and suspended-vial configuration in the case of both uncontrolled nucleation (test 14) and VISF (test 15). Residual moisture was analyzed at the end of primary drying and at different times during secondary drying. The secondary drying step was carried out using a shelf temperature of 293 K and chamber pressure 2 Pa, whereas for the test 14 and 15 was also performed at 313 K.

## RESULTS

**Freezing Behavior.** A typical temperature profile of the product, shelf and air in the chamber is shown in Figure 4a for the case of batch and suspended-vial freezing. In the case of batch freezing, the product temperature is always between the shelf temperature and the temperature of the surrounding air. In such a situation, heat is removed from the bottom, as a result of the direct contact between the shelf and the vial, but at the same time, it is supplied to the vial side by air conduction and convection, thus creating a relatively large temperature gradient within the solution.

On the other hand, in the suspended-vial configuration, heat is essentially removed from the liquid being frozen through air convection. In this case, all surfaces of the vial experience identical conditions, because the vials are immersed in air and no contact with the shelf occurs. The temperature and velocity of the surrounding air can theoretically be modulated in order to perform different freezing protocols. In this work, we used natural convection, and thus, the only processing parameter that could have been adjusted was shelf temperature. The air temperature was a result of the shelf temperature and cannot be adjusted independently. As shown in Figure 4b, the suspended-vial configuration was less efficient for a constant shelf-temperature, in terms of heat removed, that is, 0.24 vs 0.15 W. However, it should be pointed out that these results

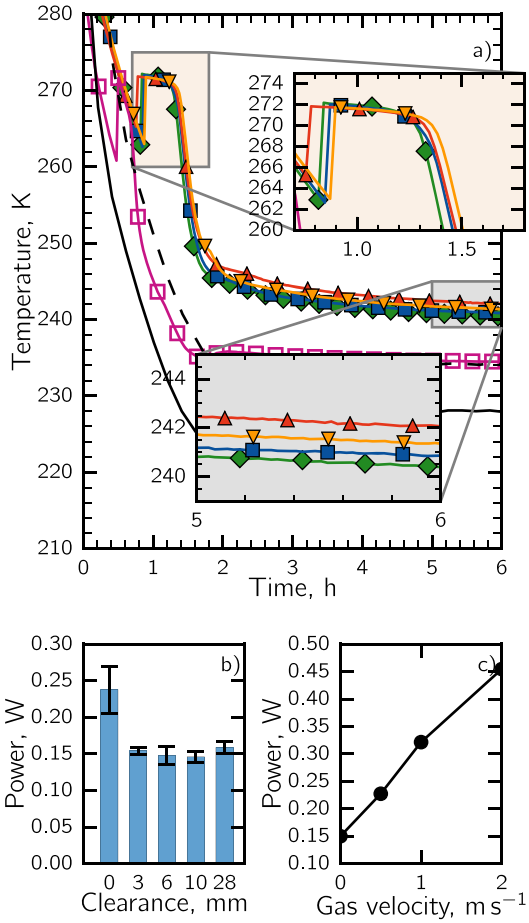


**Figure 4.** (a) Evolution of product temperature in the case of nonsuspended vials (magenta open box) and suspended vials for different clearance values: (green diamond) 3, (blue square) 6, (red triangle) 10, (yellow triangle) and 28 mm. The evolutions of shelf temperature (solid line) and that of the air (dashed line) are also shown. The average heat power removed during freezing as a function of (b) the shelf-to-vial clearance and (c) of the gas velocity.

are valid only as long as natural convection is the predominant heat transfer mechanism for the suspended-vial configuration. If forced air is used, in place of natural convection, the results could be completely different. For example, we estimated that the average heat power would increase to 0.32 W if the air velocity were set to 1 ms$^{-1}$ or 0.45 for an air velocity of 2 ms$^{-1}$, see Figure 4c. Consequently, the freezing time can be reduced by as much as 1.5 h or even more by further increasing the air velocity.

As can be seen in Figure 4b, the average heat power removed as a result of adopting suspended-vial freezing was not dependent on the vial-to-shelf clearance. As further confirmation of this result, Figure 4a shows that the temperature profile of the product during freezing was independent of the vial-to-shelf clearance for the suspended-vial configuration, at least over the 3−28 mm range. A similar result was observed for the freezing time and for the product temperature that is reached at the end of freezing.

The influence of the two freezing configurations on the morphology of the lyophilized product was also investigated. SEM images were used to evaluate their impact on the average size of the pores and their distribution, as well as on the vial-to-vial and intravial heterogeneity. An example of the results is


DOI: 10.1021/acs.iecr.8b02886
Ind. Eng. Chem. Res. 2019, 58, 1635−1649

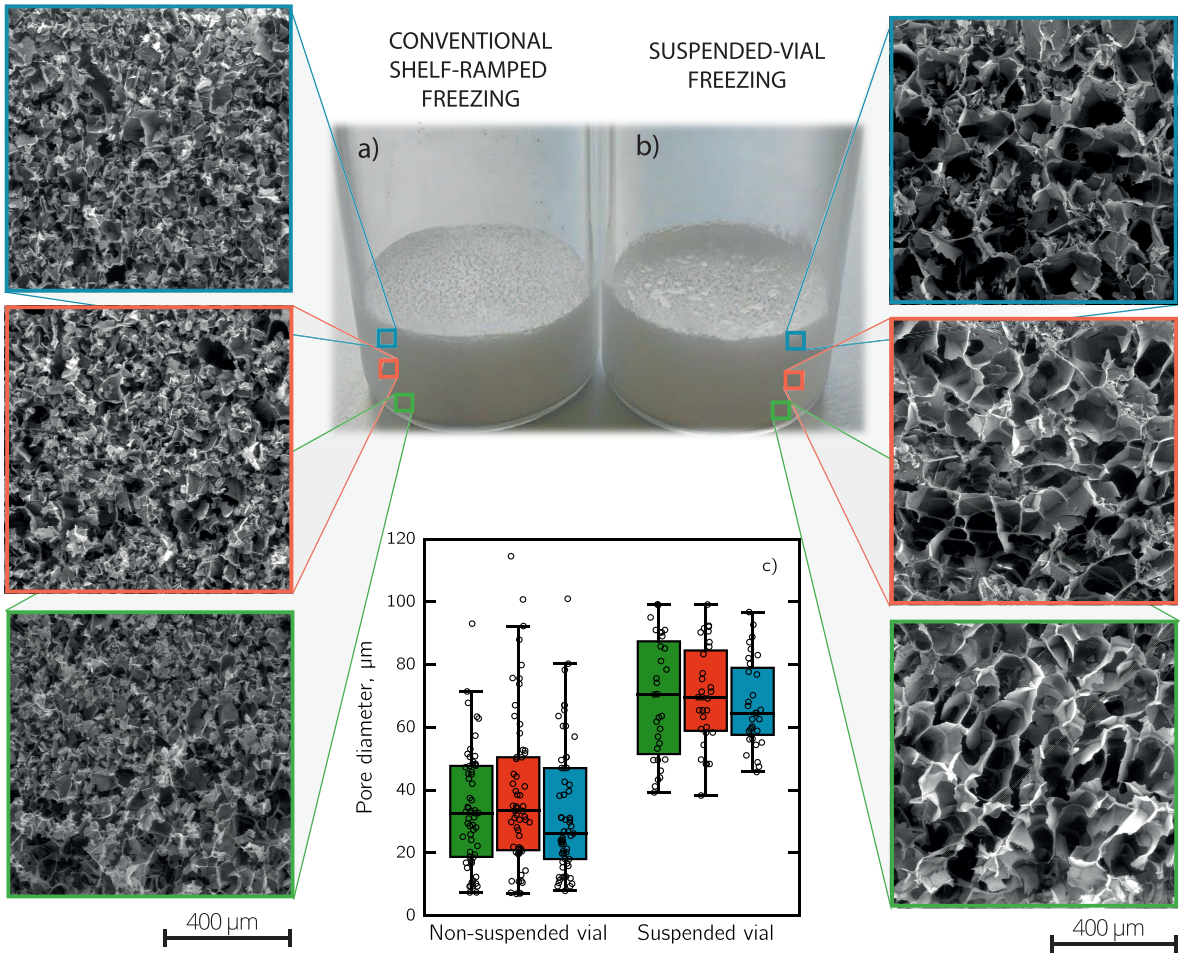


**Figure 5.** Lyophilized samples of mannitol as produced by (a) nonsuspended and (b) suspended-vial freezing. (c) Comparison of the mean pore size of a dried product, obtained by means of SEM analysis, for the case of a nonsuspended and a suspended vial configuration at different depths in the product, (green box) bottom, (red box) center, and (blue box) top. The top bar in the box plot refers to the maximum observation while the lower bar refers to the minimum observation. The top of the box refers to the third quartile, the bottom to the first quartile, the middle bar is the median value, and the bullets pertain to the original data.

shown in Figure 5. The nonsuspended freezing led to a compact structure, with pores of approximately 40 $\mu$m in diameter. Furthermore, the porous structure was not uniform as the pore size was in the 10−60 $\mu$m range, see Figure 5a. On the other hand, the suspended-vial freezing produced a more uniform porous structure, with an average size of 70 $\mu$m. This result can be confirmed from the SEM images and the pore size distributions shown in Figure 5b, which show that the pore size ranged from 65 to 80 $\mu$m. Our results suggest that suspended-vial freezing promoted crystal growth and led to a homogeneous structure made up of pores with a narrow size distribution, see Figure 5c.

Different freezing protocols have a significant impact on the product structure and on the resistance to vapor flow within the dried layer during drying ($R_p$). In Figure 6, $R_p$ is reported for a 5% mannitol solution obtained from a nonsuspended protocol (0.5 K/min as cooling rate, spontaneous nucleation), from suspended-vial freezing (spontaneous nucleation) and from VISF applied to suspended-vial freezing.

**Drying Behavior.** The heat transfer in conventional freeze-drying varies significantly according to the position of the vial within the batch, and a batch of vials is conventionally divided into five groups, Figure 7a.[49] Vials at the edge of the batch receive more heat than those located in the center, due to the

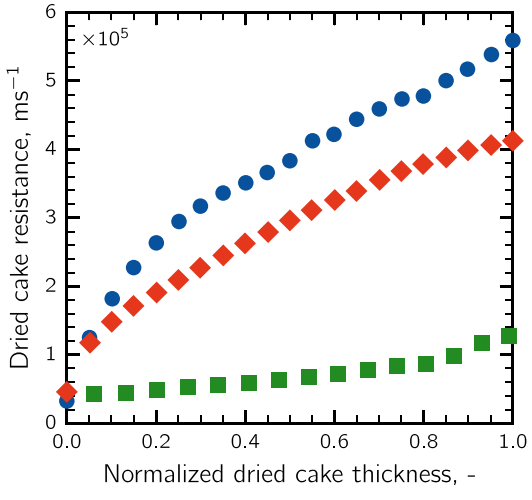


**Figure 6.** Resistance to the vapor flow in the dried layer as a function of the normalized depth of the dried layer in the case of (blue circle) nonsuspended freezing, (red diamond) suspended-vial freezing with spontaneous nucleation, and (green box) suspended-vial freezing and VISF.



DOI: 10.1021/acs.iecr.8b02886
Ind. Eng. Chem. Res. 2019, 58, 1635−1649

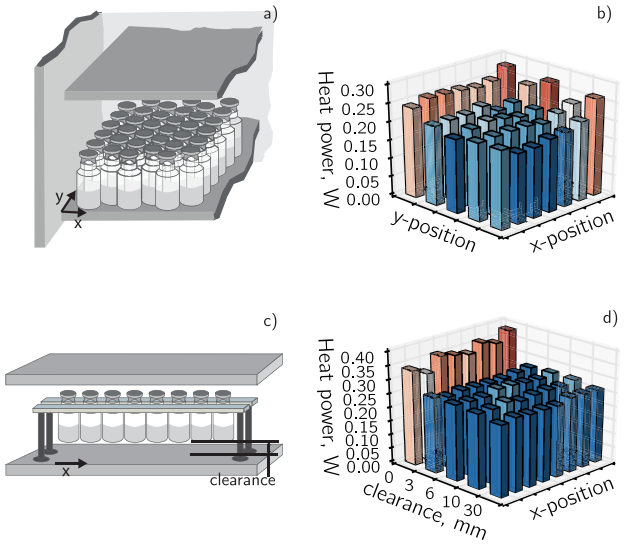


**Figure 7.** Comparison of the heat power in batch and suspended-vial freeze-drying mode. (a) Schematic of the vial positions in the chamber of a typical batch lyophilizer; (b) spatial distribution of the heat power in a batch lyophilizer; (c) schematic of the vial positions in a suspended-vial configuration; (d) spatial distribution of the heat power as a function of the clearance for a suspended-vial configuration.

contribution of radiation from the chamber walls. Figure 7b shows, as an example, the spatial distribution of heat power during primary drying, as observed experimentally. It can be observed that the heat power of the edge-vials is about 0.30 W, whereas that of central vials is approximately 0.15 W $m^{-2}$. This is typical batch freeze-drying behavior, which leads not only to remarkable differences, in terms of drying time among the vials, but is also a problem during the scale-up of a cycle or when there is a lack of control of the cycles.

On the other hand, when the configuration proposed in this work is adopted, the vials are subject to identical conditions (Figure 7c), and as a consequence, the variations in heat power between vials of the same lot are modest. It is possible to observe, in Figure 7d, that the heat power during primary drying does not depend on the clearance between the shelf and the vial bottom. In the case of vials in contact with the shelf but completely irradiated, the heat power is about 0.35 W and thus is much higher than that observed in the case of edge-vials processed in a batch freeze-dryer. In fact, the edge vials in a batch unit are partially shielded by the metallic frame or by the neighboring vials, whereas in our configuration, the vials are almost completely exposed to radiation from the chamber walls and the surrounding area. However, this configuration led to great vial-to-vial variability in the heat transfer, that is, from 0.3 to 0.4 W, because the contribution of the contact between the shelf and the vial is significant and is difficult to control. On the other hand, in the case of suspended vials, the heat power dropped to about 0.2 W, regardless of the clearance, and was surprisingly uniform, thus suggesting that, if heat is transferred predominantly by radiation, vial-to-vial uniformity will be increased and the drying time can be controlled more precisely.

The influence of the processing conditions, namely the shelf temperature and pressure, on the heat transfer was also investigated. As widely discussed in the literature, the influence of the gas temperature on the heat transfer efficiency is modest, and this analysis was therefore focused on the role of pressure. The heat power nonlinearly increased with pressure but only for the batch freeze-dryer, while it remained unchanged for the suspended-vial configuration, see Figure 8. This result was

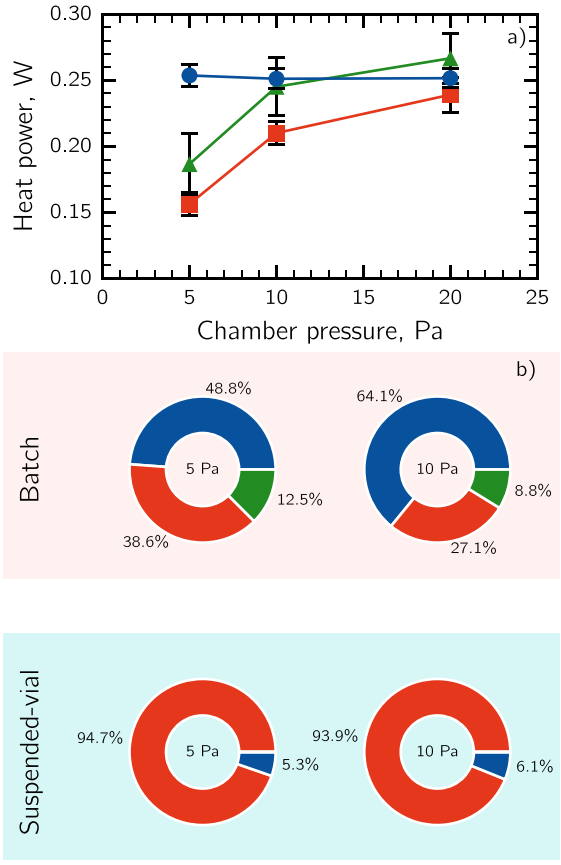


**Figure 8.** Heat power during drying as a function of pressure in the case of (blue circle) a suspended vial, (green triangle) edge-vials, and (red square) central vials in a batch lyophilizer. The relative contribution of (red square) radiation, (blue square) conduction, and (green square) direct contact to the vial-equipment heat transfer (at 5 and 10 Pa) is also shown for the batch and suspended-vial configuration.

expected, because the resistance to the heat transfer in a batch freeze-dryer is predominantly determined by conduction through the gas trapped within the gap at the bottom of the vial, which depends on the pressure.

On the other hand, in the case of the suspended-vial configuration, the heat power is almost completely independent of the pressure, because the only relevant heat transfer mechanism is radiation. Figure 8 in fact confirms that the heat power remains approximately constant over the 5−20 Pa range. Furthermore, the contribution of gas conduction to the total heat flow was approximately 5−6% for the suspend-vial configuration and in the range of 48.8%−64.1% for the batch configuration. This means that it is possible to increase the sublimation rate by decreasing the pressure as much as possible; in fact, if the pressure is reduced, the driving force for mass transfer is greater, and since the heat power is not influenced by the pressure, the sublimation rate increases.

An example of the beneficial effect of lowering the chamber pressure, in the case of suspended-vial freeze-drying, is that the drying time for 5% mannitol was found to be approximately 14



DOI: 10.1021/acs.iecr.8b02886
Ind. Eng. Chem. Res. 2019, 58, 1635−1649

h, if freeze-dried at 10 Pa and 263 K, while it was found to be 12 h at 5 Pa.

**Batch vs Suspended-Vial Freeze-Drying.** Batch and suspended-vial lyophilization were compared as far as the processing time, vial-to-vial uniformity and the maximum product temperature excursion during drying are concerned. As a first step, we investigated three plant configurations: (A) vials were loaded on the shelf in a hexagonal arrangement, (B) vials were placed in line and in contact with the shelf, and (C) vials were suspended and spontaneous nucleation was used. Configuration (C) can replicate the same heat transfer conditions as the continuous freeze-dryer proposed in this work. These tests were performed without controlling nucleation in the freezing phase. The results of this comparative analysis are shown in Table 2.

**Table 2. Comparison of Batch Freeze-Drying, Radiative with Vials in Contact and Suspended Vial Configurations Using 5% Mannitol As the Model Solution**

| test case | freeze-drying method | nucleation type | drying time, h | onset/offset, h | $T_{p,max}$, K |
|---|---|---|---|---|---|
| 1 | (A) batch | spontaneous | 22.0 | 5.2 | 257 |
| 2 | (B) contact +radiation | spontaneous | 13.2 | 1.8 | 256 |
| 3 | (C) suspended | spontaneous | 14.1 | 0.6 | 253 |
| 4 | (C) suspended | spontaneous | 10.0 | 0.7 | 256 |
| 5 | (C) suspended | spontaneous | 9.0 | 0.5 | 256 |

In the case of conventional batch freeze-drying (test 1), the drying time was found to be about 22 h, whereas this value dropped to about 14 h in the case of suspended vials performed at the same chamber pressure and shelf temperature (test 3). This occurred for two main reasons, i.e., the higher heat power and smaller mass transfer resistance to water vapor in the dried cake. As already pointed out, the heat power for the suspended vials was higher than that of the central vials in conventional freeze-drying, which represent 90% of the vials in the batch configuration. Furthermore, the suspended vial configuration produced larger pores and, thus, a smaller mass transfer resistance to the vapor flow and, consequently, a higher rate of sublimation.

Figure 9a compares the product temperature response observed for the three configurations for the constant shelf temperature and pressure. The product temperature represents an important variable that has to be controlled during the primary drying, because it needs to be maintained below a critical temperature, e.g., the collapse temperature or the API deactivation temperature.

The edge-vials showed the highest temperature in the case of conventional batch freeze-drying. Although the central vials represent more than 90% of the whole batch, the shelf temperature constraint is represented by the edge-vials, which could be overheated more easily.

When primary drying was performed at 263 K and 10 Pa, the maximum product temperature for the suspended vial configuration (test 3) was 4 K lower than that observed for the batch configuration (test 1). This means that a more aggressive cycle can be used considering a constant target for the product temperature.

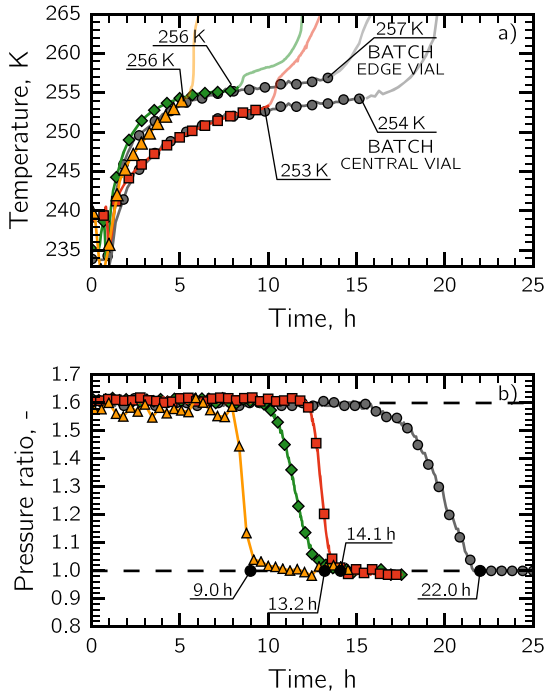


**Figure 9.** (a) Evaluation of the product temperature during primary drying and (b) the onset-offset time of the pressure ratio curve in the case of (gray circle, test 1) conventional freeze-drying, (green diamond, test 2) conventional freezing followed by the drying of vials in contact and completely irradiated, and (red square, test 3) the freezing and drying of suspended vials at $T_f$ = 263 K and $P_c$ = 10 Pa, and (yellow trangle, test 5) the freezing and drying of suspended vials at $T_f$ = 298 K and $P_c$ = 2 Pa,.

The three configurations were then compared, in terms of drying time and vial-to-vial heterogeneity, considering a constant chamber pressure and shelf temperature. The drying time was determined as the time at which the pressure ratio signal reached a plateau level. Furthermore, the difference between the onset and offset times was related to the vial-to-vial variability of the drying time. As shown in Figure 9b, the drying time of the batch configuration (test 1) was 22 h and was found to be much higher than that observed for configurations (B) and (C), that is, 13 h for the test 2 and 14 h for test 3. Moreover, we observed that the batch configuration resulted in the largest vial-to-vial drying time variability. In order to provide a quantitative estimation, the onset-offset time was found to be 5 h for the batch configuration (test 1) and only 0.6 h for the suspended vial configuration (test 3). This was due to the fact that the heat power was supplied uniformly to the vials in the suspended vial configuration, and hence, all the vials were subjected to identical heat transfer conditions, whereas in the case of conventional batch freeze-drying, the heat power supplied to the vials placed at the edge of the batch was much greater than that received by the central vials.

We compared the performances of the batch configuration and suspended-vial freeze-drying, considering a constant maximum product temperature, i.e., 257 K. In this case, the maximum product temperature was chosen merely as an example of the possible target temperatures, and it was only used to compare the performances of the two configurations. Suspended-vial freeze-drying was performed at 293 K and 4 Pa in test 4, and this resulted in a primary drying time of 10 h. In


DOI: 10.1021/acs.iecr.8b02886
Ind. Eng. Chem. Res. 2019, 58, 1635−1649

test 5, the pressure was further reduced to 2 Pa, the shelf temperature increased to 298 K, and a further reduction in drying time, i.e., 9 h, was obtained. In both cases, the product remained below the target temperature.

**VISF Applied to a Suspended-Vial Configuration.** Finally, we performed freeze-drying cycles using suspended vials coupled with VISF (configuration E). When using mannitol as the model formulation and carrying out the primary drying at 263 K and 3 Pa (test 6), the drying time was about 14 h, while the maximum temperature reached by the product during drying was only 245 K. In tests 7 and 8, the shelf temperature increased to 283 and 293 K, respectively, and the primary drying dropped to 11 and 10 h. A further increase to 313 K in the shelf temperature (test 9) decreased the primary drying duration to about 7.5 h, and only in this case product temperature reached the target temperature of 257 K, see Figure 10.

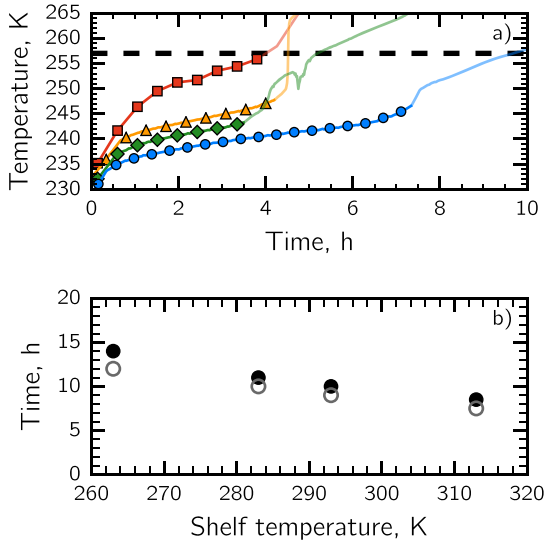


**Figure 10.** (a) Evolution of the product temperature during primary drying in the case of suspended-vial freeze-drying coupled with VISF, using (blue circle, test 6) 263 K, (green diamond, test 7) 283 K, (yellow triangle, test 8) 293 K, (red square, test 9) 313 K as the shelf temperature and 3 Pa. (b) Drying time in terms of (●) offset and (○) onset times.

This sharp reduction in drying time was possible because (a) VISF produced larger pores, and as a result the decreasing mass transfer resistance ($R_p$) and (b) the driving force to the mass transfer ($p_{w,i} - p_{w,c}$) increased as the chamber pressure decreased. Moreover, unlike the case of batch freeze-drying, lowering the chamber pressure did not affect the heat power supplied to the suspended vials, as the heat was essentially transferred by radiation; see the Drying Behavior section.

VISF applied to a suspended-vial configuration was compared with the batch mode, in the case of spontaneous and controlled nucleation; see Figure 11.

We used the LyoDriver control system for the batch cycles to optimize the cycles in line, and set 247 K as the target temperature. Test 10 consisted of a batch cycle in which spontaneous nucleation occurred, whereas nucleation was induced at 269 K using VISF in test 11. The duration of the primary drying in test 10 was about 30 h, whereas it dropped to about 19 h when VISF was used. When VISF was applied to the suspended-vial configuration, which was not in-line

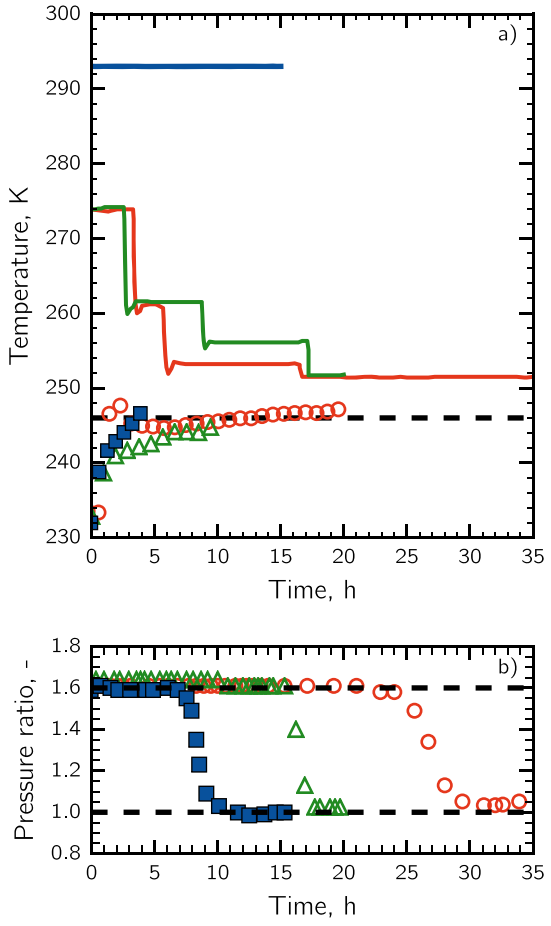


**Figure 11.** (a) Evolution of the shelf temperature (solid lines) and the product temperature (symbols); (b) Pirani/Baratron pressure ratio. (red circle and red line, test 10) batch and (green triangle and green line, test 11) VISF applied to a batch optimized in-line using the LyoDriver control system; (blue square and blue line, test 8) VISF coupled to a suspended-vial configuration ($T_s$ = 293 K, $P_c$ = 3 Pa). The target temperature was set to 247 K.

optimized, the duration of the primary drying was about 10 h and the product temperature did not exceed the target temperature. This result demonstrated that the suspended-vial configuration, together with continuous freeze-drying, is able to reduce the duration of the primary drying compared to the optimized batch cycles.

Figure 12 shows the resistance to water vapor for the three configurations, and it can be observed that VISF produces products with large open pores, and as a result, the mass transfer resistance decreases dramatically during drying. Oddone et al.[30] has already demonstrated that VISF is able to reduce vial-to-vial variability in the product structure.

**Suspended-Vial Configuration Applied to an Amorphous Excipient.** Another analysis was performed using a solution with an amorphous excipient, i.e., 5% sucrose. The process conditions for the batch (test 12) and the suspended-vial configuration (test 13 and 14) were chosen so that the product temperature did not exceed the target temperature, i.e., 240 K. In other words, tests 12 and 13 were carried out at 253 K and 10 Pa and test 14 at 273 K and 2 Pa. As shown in Table 3, the primary drying was completed in about 18 h in the case of the batch cycle, whereas, under constant process conditions, the primary drying time was 13 h for the


DOI: 10.1021/acs.iecr.8b02886
Ind. Eng. Chem. Res. 2019, 58, 1635−1649

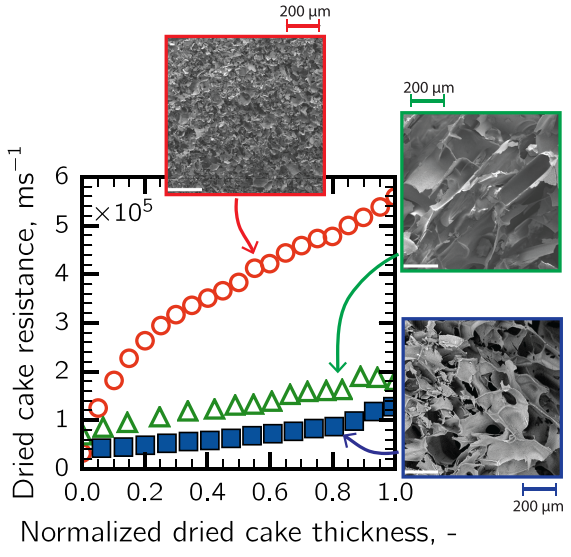


**Figure 12.** Resistance to water vapor in the case of 5% mannitol: (red circle, test 10) batch and (green triangle, test 11) VISF applied to batch; (blue blue, test 7) VISF coupled to a suspended-vial configuration.

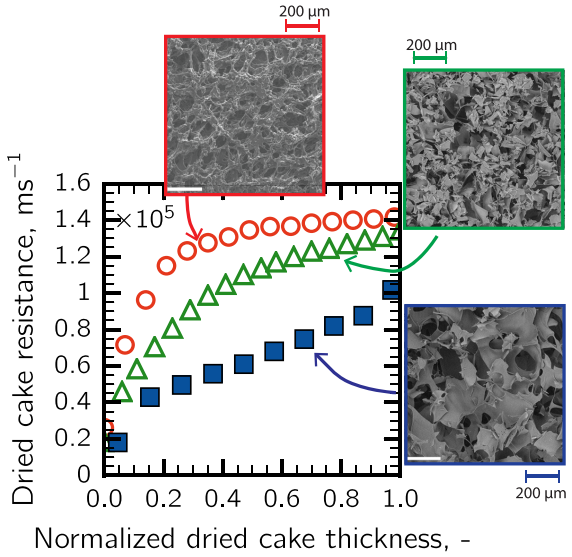


**Figure 13.** Resistance to the vapor flow in the case of 5% sucrose: (red circle, test 12) batch, (green triangle, test 14) suspended-vial and (blue square, test 15) VISF coupled to a suspended-vial configuration.

suspended-vial freeze-drying case; in test 14, by lowering the pressure to 2 Pa, we were able to conclude the primary drying after only 8.8 h. Using a suspended-vial configuration, we obtained a substantial decrease in the primary drying as a result of several factors. First, the typical edge vial effect of the batch configuration was avoided and, as a result, sublimation occurred at the maximum rate in each vial. Moreover, it was possible to further increase the sublimation rate by lowering the chamber pressure; the chamber pressure and heat transfer are essentially independent in a suspended-vial configuration. The decrease in drying time was only partially due to the much larger pore structure in the dried cake; the $R_p$ shown in Figure 13 is very similar for tests 10 and 11.

Finally, we performed a test in which VISF was coupled to a suspended-vial configuration, and a sharp reduction of 5.5 h was obtained in the drying time (test 15). Therefore, using VISF coupled with a suspended-vial configuration, it was possible to substantially decrease the drying time while avoiding the usual batch constraint and considerably increasing the sublimation rate as a result of the larger pores in the dried cake, see Figure 13.

**Secondary Drying.** The residual moisture of the sucrose-based products was measured at the end of primary drying and after 2, 4, and 6 h of secondary drying for the both batch (test 12) and suspended-vial configuration (test 14 and 15); see Figure 14.

As shown in Figure 14b, at the end of primary drying, the residual moisture observed in the central vials of the batch was 15.5%, with a standard deviation of 5.2%, whereas in the side vials was only about 9.8% with a standard deviation of 3.1%. On the other hand, the suspended-vial configuration led to a lower value of residual moisture and a substantial reduction of its variability, i.e., 8.8 ± 0.7% for spontaneous nucleation and 7.5 ± 0.3% for VISF. These results are somewhat counter-intuitive since desorption rate depends on the specific surface area of the dried matrix, and in particular, it increases as the pore size decreases. In the case of suspended-vial configuration (test 14 and 15), pore size was much higher than in the batch configuration (test 12), but the residual moisture at the end of primary drying was still much lower. This sharp reduction was due to the fact that, in the case of suspended-vial configuration, the heating surfaces entirely irradiated the vials, increasing the temperature of the dried matrix and, finally, promoting desorption already during primary drying. Contrary, in the batch configuration, chamber walls partially irradiate only side vials and not central ones.

As shown in Figure 14c, in the suspended-vial configuration, after 2 h of secondary drying carried out at 293 K and 2 Pa, the residual moisture was 4.2 ± 0.1% for both spontaneous nucleation and VISF. The residual moisture after 2 h of secondary drying carried out at 313 K was 2.4 ± 0.2% for spontaneous nucleation and 1.8 ± 0.1% for VISF. In the case of the batch configuration, after 4 h of secondary drying at 293 K and 2 Pa, the residual moisture of central vials was 4.9 ± 1.1% and 4.0 ± 0.4% for side-vials. This result demonstrated that the suspended-vial configuration was able to reduce the secondary-drying duration and the vial-to-vial variability of the residual moisture content.

In the case of the mannitol-based products, the residual moisture observed within the central vials of the batch was 3.17 ± 1.63% at the end of primary drying (test 1), whereas for

**Table 3. Comparison of Batch and Suspended-Vial Configurations in the Case of the Freeze-Drying of 5% Sucrose in 10R Vials**

| test case | freeze-drying method | nucleation type | drying time, h | onset/offset, h | $T_{p,max}$, K |
|---|---|---|---|---|---|
| 12 | (A) batch | spontaneous | 17.8 | 2.9 | 240 |
| 13 | (E) suspended | spontaneous | 13.0 | 1.1 | 240 |
| 14 | (E) suspended | spontaneous | 8.8 | 0.9 | 240 |
| 15 | (E) suspended | VISF ($T_n$ = 268 K) | 5.5 | 0.5 | 239 |



DOI: 10.1021/acs.iecr.8b02886
Ind. Eng. Chem. Res. 2019, 58, 1635−1649

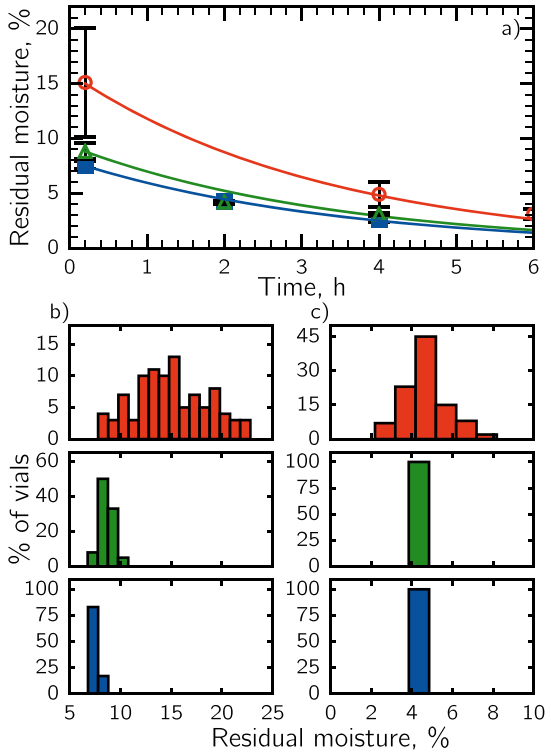


**Figure 14.** (a) Evolution of residual moisture of 5% sucrose during secondary drying; (b) residual moisture distribution within vials at the end of primary drying; and (c) at the end of secondary drying. Data refers to sucrose solutions in the case of (red circle and red line, test 12) batch, (green triangle and green line, test 14) suspended-vial and (blue square and blue line, test 15) VISF coupled to a suspended-vial configuration.

the suspended-vial configuration (test 9) was 1.01 ± 0.28%. Assuming that the residual moisture target was 1%, several hours of secondary drying is still needed in batch configuration,[61] whereas it can be skipped in the case of suspended-vial configuration, which makes it possible to further reduce the total cycle time.

## CONCLUSIONS AND FUTURE PERSPECTIVES

A new pharmaceutical freeze-drying concept, which makes it possible to move from batch to continuous manufacturing, has been proposed. The continuous flow of vials is achieved by suspending them over a moving track. The vials move through chambers which have different pressure and temperature conditions and are separated by a load-lock system.

In order to obtain a quantitative estimation of the advantages of the proposed continuous strategy, with respect to the batch one, a functional version of the continuous plant has been set up. This plant allowed us to simulate the same heat transfer conditions to which vials would be exposed in a continuous lyophilizer. The performances of the batch and continuous configurations were evaluated in terms of processing time and vial-to-vial variability.

We have demonstrated that suspended vial freezing leads to a final product which has a larger and more uniform pore structure than that obtained with conventional freezing, which makes the drying step faster.

The suspended vial configuration has allowed a more accurate control of the heat input, which is transferred uniformly to all of the vials being processed. Furthermore, the freeze-drying of suspended vials has led to a reduction in the drying time and in the onset-offset time. To provide an example, the primary drying time was approximately 3−4 times shorter than that observed for the batch lyophilizer. The total cycle time is much shorter (approximately 6 times) if we consider that some time-consuming operations, such as filling, are carried out in parallel to the process and, thus, do not contribute to increase the cycle time. We have also estimated that, if lyophilization operates in continuous mode, the equipment would be 6−8 times smaller than a batch lyophilizer. This comparison has been done on constant throughput.

The obtained results have demonstrated the feasibility of our concept as a valid alternative to conventional batch freeze-drying, which may open up new perspectives and opportunities to completely rethink the production of parenteral products and make freeze-drying more efficient and versatile.

## ASSOCIATED CONTENT

### Supporting Information

The Supporting Information is available free of charge on the ACS Publications website at DOI: 10.1021/acs.iecr.8b02886.

Equations used to estimate the resistance to heat and mass transfer for the two process configurations, batch and continuous lyophilization (PDF)

## AUTHOR INFORMATION

### Corresponding Author

*E-mail: roberto.pisano@polito.it.

### ORCID

Luigi C. Capozzi: 0000-0002-3046-9876
Bernhardt L. Trout: 0000-0003-1417-9470
Roberto Pisano: 0000-0001-6990-3126

### Notes

The authors declare no competing financial interest.

## LIST OF SYMBOLS

$P_c$ chamber pressure, Pa
$p_{w,c}$ partial pressure of the water in the drying chamber, Pa
$p_{w,i}$ partial pressure of the water at the sublimating interface, Pa
$R_p$ resistance of the dried layer to the vapor flow, m $s^{-1}$
$T$ temperature, K
$T_n$ nucleation temperature, K
$T_p$ temperature of the product, K
$T_s$ shelf temperature, K
$T_{s,n}$ holding temperature before the induction of nucleation, K
$T_{s,m}$ holding temperature after the induction of nucleation, K

## REFERENCES

(1) Harrington, T. S.; Alinaghian, L.; Srai, J. S. Making the business case for continuous manufacturing in the pharmaceutical industry. Proceedings of the 25th Annual Production and Operations Management Society Conference, May 9−12, 2014, Atlanta, GA.

(2) Allison, G.; Cain, Y. T.; Cooney, C.; Garcia, T.; Bizjak, T. G.; Holte, O.; Jagota, N.; Komas, B.; Korakianiti, E.; Kourti, D. Regulatory and quality considerations for continuous manufacturing. May 20−21, 2014 Continuous Manufacturing Symposium. *J. Pharm. Sci.* **2015**, *104*, 803−812.

(3) Woodcock, J. *Modernizing pharmaceutical manufacturing-Continuous Manufacturing as a key enabler*. International Symposium



DOI: 10.1021/acs.iecr.8b02886
*Ind. Eng. Chem. Res.* 2019, 58, 1635−1649

on Continuous Manufacturing of Pharmaceuticals, May 20−21, 2014, MIT, Cambridge, MA, USA.
(4) FDA, *Advancement of Emerging Technology Applications to Modernize the Pharmaceutical Manufacturing Base Guidance for Industry*; Draft guidance, 2015.
(5) Lee, S. Present and future for continuous manufacturing: FDA perspective. Proceedings of the 3rd FDA/PQRI Conference on Advancing Product Quality, March 22−24, 2017, Rockville, MD, USA.
(6) Subcommittee for Advanced Manufacturing of the National Science and Technology Council, *Advanced Manufacturing: A Snapshot of Priority Technology Areas Across the Federal Government*; Report, 2016.
(7) Hernán, D. Continuous manufacturing: challenges and opportunities. EMA perspective. Proceedings of the 3rd FDA/PQRI Conference on Advancing Product Quality, March 22−24, 2017, Rockville, MD, USA.
(8) Matsuda, Y. Continuous Manufacturing: PMDA Perspective. International Symposium on Continuous Manufacturing of Pharmaceuticals, September 26−27, 2016, MIT, Cambridge, MA, USA.
(9) Leuenberger, H. New trends in the production of pharmaceutical granules: batch versus continuous processing. *Eur. J. Pharm. Biopharm.* **2001**, *52*, 289−296.
(10) Plumb, K. Continuous processing in the pharmaceutical industry: changing the mind set. *Chem. Eng. Res. Des.* **2005**, *83*, 730−738.
(11) Byrn, S.; Futran, M.; Thomas, H.; Jayjock, E.; Maron, N.; Meyer, R. F.; Myerson, A. S.; Thien, M. P.; Trout, B. L. Achieving continuous manufacturing for final dosage formation: Challenges and how to meet them. May 20−21, 2014 Continuous Manufacturing Symposium. *J. Pharm. Sci.* **2015**, *104*, 792−802.
(12) Schaber, S. D.; Gerogiorgis, D. I.; Ramachandran, R.; Evans, J. M.; Barton, P. I.; Trout, B. L. Economic analysis of integrated continuous and batch pharmaceutical manufacturing: a case study. *Ind. Eng. Chem. Res.* **2011**, *50*, 10083−10092.
(13) McKenzie, P.; Kiang, S.; Tom, J.; Rubin, A. E.; Futran, M. Can pharmaceutical process development become high tech? *AIChE J.* **2006**, *52*, 3990−3994.
(14) Poechlauer, P.; Manley, J.; Broxterman, R.; Gregertsen, B.; Ridemark, M. Continuous processing in the manufacture of active pharmaceutical ingredients and finished dosage forms: an industry perspective. *Org. Process Res. Dev.* **2012**, *16*, 1586−1590.
(15) Cole, K. P.; Groh, J. M.; Johnson, M. D.; Burcham, C. L.; Campbell, B. M.; Diseroad, W. D.; Heller, M. R.; Howell, J. R.; Kallman, N. J.; Koenig, T. M.; May, S. A.; Miller, R. D.; Mitchell, D.; Myers, D. P.; Myers, S. S.; Phillips, J. L.; Polster, C. S.; White, T. D.; Cashman, J.; Hurley, D.; Moylan, R.; Sheehan, P.; Spencer, R. D.; Desmond, K.; Desmond, P.; Gowran, O. Kilogram-scale prexasertib monolactate monohydrate synthesis under continuous-flow CGMP conditions. *Science* **2017**, *356*, 1144−1150.
(16) Yu, L. Continuous manufacturing has a strong impact on drug quality. *FDA Voice*. April 12, 2016.
(17) Jessen, V. Continuous manufacturing, A qualitative analysis of challenges and opportunities for introducing continuous manufacturing in pharmaceutical companies. Proceedings of the ISPE Network Meeting - Biotechnology CoP. Continuous Manufacturing, June 16, 2016, Bagsværd, Denmark.
(18) Tezyk, M.; Milanowski, B.; Ernst, A.; Lulek, J. Recent progress in continuous and semi-continuous processing of solid oral dosage forms: a review. *Drug Dev. Ind. Pharm.* **2016**, *42*, 1195−1214.
(19) Heider, P. L.; Born, S. C.; Basak, S.; Benyahia, B.; Lakerveld, R.; Zhang, H.; Hogan, R.; Buchbinder, L.; Wolfe, A.; Mascia, S. Development of a multi-step synthesis and workup sequence for an integrated, continuous manufacturing process of a pharmaceutical. *Org. Process Res. Dev.* **2014**, *18*, 402−409.
(20) Hernandez, R. Continuous manufacturing: a changing processing paradigm. *BioPharm. International* **2015**, *28*, 20−27.
(21) Barresi, A. A.; Pisano, R.; Fissore, D.; Rasetto, V.; Velardi, S. A.; Vallan, A.; Parvis, M.; Galan, M. Monitoring of the primary drying of a lyophilization process in vials. *Chem. Eng. Process.* **2009**, *48*, 408−423.
(22) Fissore, D.; Pisano, R.; Barresi, A. A. Monitoring of the secondary drying in freeze-drying of pharmaceuticals. *J. Pharm. Sci.* **2011**, *100*, 732−742.
(23) Pisano, R.; Fissore, D.; Barresi, A. A. A new method based on the regression of step response data for monitoring a freeze-drying cycle. *J. Pharm. Sci.* **2014**, *103*, 1756−1765.
(24) Pisano, R.; Fissore, D.; Barresi, A. A. Noninvasive monitoring of a freeze-drying process for tert-butanol/water cosolvent-based formulations. *Ind. Eng. Chem. Res.* **2016**, *55*, 5670−5680.
(25) De Beer, T.; Vercruysse, P.; Burggraeve, A.; Quinten, T.; Ouyang, J.; Zhang, X.; Vervaet, C.; Remon, J. P.; Baeyens, W. In-line and real-time process monitoring of a freeze drying process using Raman and NIR spectroscopy as complementary process analytical technology (PAT) tools. *J. Pharm. Sci.* **2009**, *98*, 3430−3446.
(26) Oddone, I.; Fulginiti, D.; Barresi, A. A.; Grassini, S.; Pisano, R. Non-invasive temperature monitoring in freeze drying: control of freezing as a case study. *Drying Technol.* **2015**, *33*, 1621−1630.
(27) Fissore, D.; Pisano, R.; Barresi, A. A. Process analytical technology for pharmaceutical freeze-drying monitoring: a review. *Drying Technol.* **2018**, *36*, 1839.
(28) De Beer, T.; Wiggenhorn, M.; Hawe, A.; Kasper, J.; Almeida, A.; Quinten, T.; Friess, W.; Winter, G.; Vervaet, C.; Remon, J. P. Optimization of a pharmaceutical freeze-dried product and its process using an experimental design approach and innovative process analyzers. *Talanta* **2011**, *83*, 1623−1633.
(29) Pisano, R.; Fissore, D.; Barresi, A. A.; Brayard, P.; Chouvenc, P.; Woinet, B. Quality by design: optimization of a freeze-drying cycle via design space in case of heterogeneous drying behavior and influence of the freezing protocol. *Pharm. Dev. Technol.* **2013**, *18*, 280−295.
(30) Oddone, I.; Van Bockstal, P.-J.; De Beer, T.; Pisano, R. Impact of vacuum-induced surface freezing on inter-and intra-vial heterogeneity. *Eur. J. Pharm. Biopharm.* **2016**, *103*, 167−178.
(31) Goshima, H.; Do, G.; Nakagawa, K. Impact of ice morphology on design space of pharmaceutical freeze-drying. *J. Pharm. Sci.* **2016**, *105*, 1920−1933.
(32) Lim, J. Y.; Kim, N. A.; Lim, D. G.; Kim, K. H.; Choi, D. H.; Jeong, S. H. Process cycle development of freeze drying for therapeutic proteins with stability evaluation. *J. Pharm. Invest.* **2016**, *46*, 519−536.
(33) Patel, S. M.; Pikal, M. J. Emerging freeze-drying process development and scale-up issues. *AAPS PharmSciTech* **2011**, *12*, 372−378.
(34) Lee, S. L.; O'Connor, T. F.; Yang, X.; Cruz, C. N.; Chatterjee, S.; Madurawe, R. D.; Moore, C. M.; Lawrence, X. Y.; Woodcock, J. Modernizing pharmaceutical manufacturing: from batch to continuous production. *J. Pharm. Innov.* **2015**, *10*, 191−199.
(35) Patel, S. M.; Nail, S. L.; Pikal, M. J.; Geidobler, R.; Winter, G.; Hawe, A.; Davagnino, J.; Gupta, S. R. Lyophilized drug product cake appearance: what is acceptable? *J. Pharm. Sci.* **2017**, *106*, 1706−1721.
(36) Rey, L. *Freeze-drying/lyophilization of pharmaceutical and biological products*; CRC Press: New York, 2016.
(37) Rhian, M.; Maister, H.; Hutton, R. A continuous freeze drier for laboratory studies. *Appl. Microbiol.* **1957**, *5*, 323.
(38) Van der Wel, P. Active Freeze Drying. Proceedings of 5th European Drying Conference, October 21−23, 2015, Budapest, Hungary.
(39) Bullich, R. Continuous Freeze Drying. PharmaProcess Forum, October 2−6, 2015, Barcelona, Spain.
(40) Corver, J. A. W. M. Method and system for freeze-drying injectable compositions, in particular pharmaceutical compositions. U.S. Patent US20140215845 A1, 2012.
(41) De Meyer, L.; Van Bockstal, P.-J.; Corver, J.; Vervaet, C.; Remon, J.; De Beer, T. Evaluation of spin freezing versus conventional freezing as part of a continuous pharmaceutical freeze-drying concept for unit doses. *Int. J. Pharm.* **2015**, *496*, 75−85.


DOI: 10.1021/acs.iecr.8b02886
*Ind. Eng. Chem. Res.* 2019, 58, 1635−1649

(42) Pisano, R.; Barresi, A. A.; Capozzi, L. C.; Novajra, G.; Oddone, I.; Vitale-Brovarone, C. Characterization of the mass transfer of lyophilized products based on X-Ray micro-computed tomography images. *Drying Technol.* **2017**, *35*, 933−938.
(43) Capozzi, L. C.; Pisano, R. Looking inside the 'black box': Freezing engineering to ensure the quality of freeze-dried biopharmaceuticals. *Eur. J. Pharm. Biopharm.* **2018**, *129*, 58−65.
(44) Peters, B.-H.; Staels, L.; Rantanen, J.; Molnár, F.; De Beer, T.; Lehto, V.-P.; Ketolainen, J. Effects of cooling rate in microscale and pilot scale freeze-drying-Variations in excipient polymorphs and protein secondary structure. *Eur. J. Pharm. Sci.* **2016**, *95*, 72−81.
(45) Oddone, I.; Pisano, R.; Bullich, R.; Stewart, P. Vacuum-Induced nucleation as a method for freeze-drying cycle optimization. *Ind. Eng. Chem. Res.* **2014**, *53*, 18236−18244.
(46) Searles, J. A.; Carpenter, J. F.; Randolph, T. W. The ice nucleation temperature determines the primary drying rate of lyophilization for samples frozen on a temperature-controlled shelf. *J. Pharm. Sci.* **2001**, *90*, 860−871.
(47) Tang, X. C.; Pikal, M. J. Design of freeze-drying processes for pharmaceuticals: practical advice. *Pharm. Res.* **2004**, *21*, 191−200.
(48) Pisano, R.; Capozzi, L. C. Prediction of product morphology of lyophilized drugs in the case of Vacuum Induced Surface Freezing. *Chem. Eng. Res. Des.* **2017**, *125*, 119−129.
(49) Pisano, R.; Barresi, A. A.; Fissore, D. *Heat transfer in freeze-drying apparatus*; Intech: Rijeka, 2011; pp 91−114.
(50) Ganguly, A.; Nail, S. L.; Alexeenko, A. Experimental determination of the key heat transfer mechanisms in pharmaceutical freeze-drying. *J. Pharm. Sci.* **2013**, *102*, 1610−1625.
(51) Pikal, M.; Roy, M.; Shah, S. Mass and heat transfer in vial freeze-drying of pharmaceuticals: Role of the vial. *J. Pharm. Sci.* **1984**, *73*, 1224−1237.
(52) Scutellà, B.; Passot, S.; Bourlés, E.; Fonseca, F.; Tréléa, I. C. How vial geometry variability influences heat transfer and product temperature during freeze-drying. *J. Pharm. Sci.* **2017**, *106*, 770−778.
(53) Rambhatla, S.; Pikal, M. J. Heat and mass transfer scale-up issues during freeze-drying, I: atypical radiation and the edge vial effect. *AAPS PharmSciTech* **2003**, *4*, 22−31.
(54) Pikal, M. J.; Bogner, R.; Mudhivarthi, V.; Sharma, P.; Sane, P. Freeze-drying process development and scale-up: scale-up of edge vial versus center vial heat transfer coefficients, Kv. *J. Pharm. Sci.* **2016**, *105*, 3333−3343.
(55) Barresi, A. A.; Pisano, R.; Rasetto, V.; Fissore, D.; Marchisio, D. L. Model-based monitoring and control of industrial freeze-drying processes: effect of batch nonuniformity. *Drying Technol.* **2010**, *28*, 577−590.
(56) Gan, K. H.; Bruttini, R.; Crosser, O. K.; Liapis, A. I. Freeze-drying of pharmaceuticals in vials on trays: effects of drying chamber wall temperature and tray side on lyophilization performance. *Int. J. Heat Mass Transfer* **2005**, *48*, 1675−1687.
(57) Gan, K. H.; Crosser, O.; Liapis, A.; Bruttini, R. Lyophilization in vials on trays: Effects of tray side. *Drying Technol.* **2005**, *23*, 341−363.
(58) Cheng, H.-P.; Tsai, S.-M.; Cheng, C.-C. Analysis of heat transfer mechanism for shelf vacuum freeze-drying equipment. *Adv. Mater. Sci. Eng.* **2014**, *2014*, 1.
(59) Alexeenko, A. A.; Ganguly, A.; Nail, S. L. Computational analysis of fluid dynamics in pharmaceutical freeze-drying. *J. Pharm. Sci.* **2009**, *98*, 3483−3494.
(60) Rasetto, V.; Marchisio, D. L.; Fissore, D.; Barresi, A. A. On the use of a dual-scale model to improve understanding of a pharmaceutical freeze-drying process. *J. Pharm. Sci.* **2010**, *99*, 4337−4350.
(61) Oddone, I.; Barresi, A. A.; Pisano, R. Influence of controlled ice nucleation on the freeze-drying of pharmaceutical products: the secondary drying step. *Int. J. Pharm.* **2017**, *524*, 134−140.


DOI: 10.1021/acs.iecr.8b02886
*Ind. Eng. Chem. Res.* 2019, 58, 1635−1649